Silver Colloidal Effects on Excited-State Structure and Intramolecular Charge Transfer of *p*-N,N-Dimethylaminobenzoic Acid in Aqueous Cyclodextrin Solutions

Jungkwon Choi, Yanghee Kim, Minjoong Yoon,* Seung Joon Lee,† Kwan Kim,† and Sae Chae Jeoung‡

Department of Chemistry, Chungnam National University, Taejon 305-764, Korea
†Department of Chemistry and Center for Molecular Catalysis, Seoul National University, Seoul 151-742, Korea
‡Spectroscopy Laboratory, Korea Research Institute of Standards and Science, Taejon 305-764, Korea
Received October 12, 2000

The silver colloidal effects on the excited-state structure and intramolecular charge transfer (ICT) of *p*-N,N-dimethylaminobenzoic acid (DMABA) in aqueous cyclodextrin (CD) solutions have been investigated by UV-VIS absorption, steady-state and time-resolved fluorescence, and transient Raman spectroscopy. As the concentration of silver colloids increases, the ratio of the ICT emission to the normal emission (I_a/I_b) of DMABA in the aqueous α-CD solutions are greatly decreased while the I_a/I_b values in the aqueous β-CD solutions are significantly enhanced. It is also noteworthy that the ICT emission maxima are red-shifted by 15-40 nm upon addition of silver colloids, implying that DMABA encapsulated in α-CD or β-CD cavity is exposed to more polar environment. The transient resonance Raman spectra of DMABA in silver colloidal solutions demonstrate that DMABA in the excited-state is desorbed from silver colloidal surfaces as demonstrated by the disappearance of $\nu_s(CO_2^-)$(1380 cm^{-1}) with appearance of ν(C-OH)(1280 cm^{-1}) band, respectively. Thus, in the aqueous β-CD solutions the carboxylic acid group of DMABA in the excited-state can be readily hydrogen-bonded with the secondary hydroxyl group of β-CD while in aqueous and α-CD solutions the carboxylic acid group of DMABA has the hydrogen-bonding interaction with water. Consequently, in the aqueous β-CD solutions the enhancement of the I_a/I_b value arises from the intermolecular hydrogen-bonding interaction between DMABA and the secondary hydroxyl group of β-CD as well as the lower polarity of the rim of the β-CD cavity compared to bulk water. This is also supported by the increase of the association constant for DMABA/β-CD complex in the presence of silver colloids.

Keywords : *p*-N,N-Dimethylaminobenzoic acid, Intramolecular charge transfer, Cyclodextrin silver colloidal effects.

Introduction

In recent years, the photoinduced intramolecular charge transfer (ICT) in the aqueous cyclodextrin (CD) solutions has been observed for various organic molecules such as *p*-N,N-dimethylaminobenzoic acid (DMABA),[1-3] *p*-N,N-diethylaminobenzoic acid (DEABA)[4] and *p*-N,N-dimethylaminobenzonitrile (DMABN).[5-7] In aqueous solutions, the cyclodextrin which is the cyclic polymers of α-, β- or γ-amylose forms a very well-defined hydrophobic cavity and encapsulates a suitable molecule. The resulting supramolecules often exhibit properties drastically different from those of the free guest molecules in the aqueous solutions. The α-, β- and γ-cyclodextrin contain six, seven and eight amylose units, forming the diameter of the inner rim of the cavities approximately 4.5, 6.5 and 8 Å, respectively. The interior of the CD cavity is relatively nonpolar while the rims are moderately polar due to the hydroxyl groups and nearby water molecules. Thus, the main aim of studying the ICT process in CD solutions was to find out how the cavity affects the ICT state and whether it is due to the reduced polarity of the cavity or to the restrictions imposed on the molecular motions in the CD cavity.

In 1994, Jiang reported that the conjugate base form of DMABA in aqueous solutions had a higher relative population of the ICT state and a stronger excitation wavelength dependence of ICT fluorescence than the acid form.[1,3] Furthermore, he observed the effects of α-CD and β-CD on the ICT of DMABA in aqueous solutions, reporting that the dimethylamino group of DMABA molecule is included in the α-CD and β-CD cavity and the ratio of the ICT emission to the normal emission increased as α-CD or β-CD concentration increases. However, he did not consider the hydrogen-bonding interaction of the carboxylic acid of DMABA and water on the ICT process. In 1995, Yoon *et al.* demonstrated that the specific hydrogen-bonding between the carboxylic acid group of DMABA and water in aqueous CD solutions played an important role in the formation of an ICT state.[2] From the time-resolved fluorescence spectroscopic results, the complexation pattern of DMABA/β-CD was found to be quite different from that of DMABA/α-CD. They also observed SiO_2 colloidal effects on the excited-state ICT process of DMABA in acetonitrile, demonstrating that the formation of the ICT state was enhanced by the hydrogen-bonding between the carboxylic acid group of DMABA and the SiO_2 colloidal surface while the hydrogen-bonding between the amino group of DMABA and the SiO_2 colloidal surface inhibited the formation of the ICT state.[8]

As discussed above, the fluorescence spectroscopic studies on ICT process in the cyclodextrin solution was widely attempted. However, their studies do not give a clear understanding of the molecular structure in the excited-ICT state, even though a limited IR studies have been done to explore the structure and dynamics of the excited electronic states of DMABN in polar and nonpolar solvents by Hamaguchi *et al.*.[9] They reported that both the singlet and triplet ICT state showed large downshifts (>120 cm^{-1}) of the $C \equiv N$ stretch frequency, indicating that the charge transfer had a significant effect on the structure of the cyano group. Nevertheless, no evidence of the conformational change in the electron donating amino group was not yet observed. In this point of view, it is necessary to extend the conformational studies by using Raman scattering.[10] However, the ordinary Raman spectroscopy is not suitable for the organic molecules such as DMABA showing a strong ICT emission. Thus, the surface enhanced resonance Raman scattering technique (SERS), which use the silver colloids as an active site to enhance the Raman signal to overcome the fluorescence is useful method to determine the structure of molecules adsorbed on certain surface in the ground state. Moskovits *et al.* investigated the spectra of *p*-aminobenzoic acid (PABA) adsorbed on aqueous silver colloidal particles, reporting the PABA molecule was deduced to be adsorbed flat on the surface, π-bonding through the benzen ring.[11] Suh *et al.* observed the SERS spectra of isomeric pyridinecarboxylic acids, *o*- and *p*-aminobenzoic acids, thiosalicylic and 4-methylthiobenzoic acids.[12] Furthermore, the transient resonance Raman spectroscopy is established as powerful tool for studying the structure of electronically excited molecules.[13-16] The transient resonance Raman spectroscopy, however, is not suitable for the organic molecules such as DMABA and its derivatives, which show a strong ICT emission. From this point of view, the silver colloids, which display the absorption band at the longer wavelength with adsorbate, are useful materials for the observation of the structure of adsorbate in the excited-state.

Thus it is quite necessary to obtain the optical properties of DMABA/CD in the presence of silver colloids. In this paper the silver colloidal effects on excited-state ICT process and structure of DMABA in aqueous CD solutions have been investigated by UV-VIS absorption, steady-state and time-resolved fluorescence, and the transient resonance Raman spectroscopy.

Experimental Section

p-N,N-dimethylaminobenzoic acid (DMABA), $AgNO_3$ and sodium borohydride were purchased from Aldrich Chemical Co.

The silver colloidal particles were prepared according to the recipe reported by Creighton.[17] A 60 mL solution of 2×10^{-3} M sodium borohydride was mixed with a 22 ± 2 mL solution of 1×10^{-3} M $AgNO_3$; both solutions were chilled at ice temperature. The silver colloids appeared pale yellow. Freshly prepared silver colloidal suspensions were stable for a month when stored in the dark. The particle size of silver colloid was determined *ca.* 200 Å by transmission electron microscopy (Carl Zeiss; Model EM912 Omega). The number of silver molecules per colloidal particle was 2.4×10^5.

The absorption spectra were measured on a Cary 3E UV-VIS spectrophotometer. The steady-state fluorescence spectra were recorded on a scanning SLM AMINCO 4800 spectrofluorometer which makes it possible to obtain corrected spectra using Rhodamine B as a quantum counter. The solutions were accurately diluted with the proper solvent to have an optical density not to exceed 0.6 at the excitation wavelength to eliminate the self-absorption effect.

We have attempted to obtain the infrared spectra of DMABA adsorbed on silver colloidal particles for a better interpretation of its ICT emission on colloidal surfaces. However, since the concentration of colloidal solutions was too dilute to record the infrared spectra, we have recorded the infrared spectra of DMABA that has been self-assembled on commercially available Ag (Aldrich, 99.9+%, 2-3.5 μm) powders by means of a diffuse reflectance infrared Fourier transform (DRIFT) spectroscopy. These powdered samples were transferred to a 4 mm diameter cup (Harrick microsampling cup) without compression. After leveling by trapping the cup gently, the samples were subjected to DRIFT analysis. DRIFT spectra were measured with a Bruker IFS 113v Fourier transform IR spectrometer equipped with a globar light source, a liquid N_2-cooled wide-band mercury cadmium telluride detector, and a Harrick Model DRA-3CI diffuse reflectance accessory. A total of 128 scans were measured in the range 3500-1000 cm^{-1} at a resolution of 4 cm^{-1} with the use of previously scanned pure silver powder as the background. The Happ-Genzel apodization function was used in Fourier transforming all the interferograms.

Raman spectra of DMABA in NaOH solutions (pH=13) and solid DMABA were obtained with a Renishaw Ramascope system 2000 using the 514.5 nm line of an Ar ion laser (Spectra Physics mode 163-C4210) as an exciting source. Glass capillary tube was used as sampling device and Raman scattering was observed with 180° back scattering geometry. The surface enhanced Raman scattering spectra were obtained using a 514.5 nm line of an Ar ion laser (Lexel 3500-7) as an exciting source. The Raman scattering signal was collected by a Spex 1404 double monochromator and LN_2 cooled CCD arrary detector (Spex Spectrum One).

The transient resonance Raman spectra on DMABA adsorbed on silver particles in aqueous α-CD and β-CD solutions were obtained by the probe pulse at 468 nm and the pump pulse at 435 nm, respectively. The 468 nm and 435 nm were prepared from the first anti-Stokes shifted Raman lines of H_2, excited by the 532 nm pluses from nanosecond Q-switched Nd: YAG laser. The transient resonance Raman scattering signal was collected by a HR 640 spectrograph (Jovin-Yvon) connected with a delay generator (Stanford Research DG 535), a pulse generator (Princeton Instrument FG 135), and a gated intensifited photodiode array detector (Princeton Instrument IRY 700). The sample solutions were flowed through a glass capillary (0.8 mm i.d.) at rate sufficient to ensure that each pluse encounted a fresh volume of sample.

Fluorescence lifetimes of DMABA in the semiconductor colloidal solutions were measured by a time-correlated single photon counting (TCSPC) method, employing a dual-jet picosecond dye laser (Coherent; Model 702) synchronously pumped by a mode-locked Ar ion laser (Coherent; Innova 200). The cavity-dumped beam from the dye laser had 1 ps pulse width, average power of 100 mW at 3.8 MHz dumping rate and a tunability of 560-620 nm by using Rhodamine 6G as a gain dye and DODCI (diethoxydicyanineiodide) as a saturable absorber. To excite the sample, the laser pulse was frequency-doubled by β-BBO (β-barium borate) crystal. All the standard electronics used for the TCSPC were from EG & G Ortec. This method allows a time resolution of about 10 ps after deconvolution.

Results and Discussion

Figure 1a shows the absorption spectra of DMABA in aqueous solutions with different concentration of silver colloids. Upon increasing the concentration of silver colloids, the absorption maxima around 310 nm was blue-shifted with gradual increase in the absorbance, followed by the appearance of new absorption band around 600 nm. The new absorption band is attributed to the formation of the DMABA/silver colloid complex by the charge transfer interaction. In contrast to the dramatic changes in the absorption spectra, the fluorescence spectra of DMABA are little affected by the presence of silver colloids as shown in Figure 1b. The intensity of the emission is slightly increased by the presence of silver colloids and the normal emission maxima are blue-shifted. This emission spectrum in the presence of silver colloids is consistent with the emission spectrum of DMABA in high pH buffer solutions, indicating that DMABA is adsorbed on silver colloidal surface as a carboxylate form.

In order to further understand the interaction and binding form of DMABA with silver colloidal particles in the ground-state, we have measured the DRIFT and Raman scattering spectra of DMABA adsorbed on silver particles. The most prominent features for neat DMABA in DRIFT spectra (Figure 2(a)) are a band at 1668 cm^{-1} due to C=O stretching, a band at 945 cm^{-1} due to a symmetric stretching of an amine group (ν_s(NC$_2$)), and a band at 1190 cm^{-1} due to an asymmetric stretching of an amine group (ν_{as}(NC$_2$)). In case of DMABA adsorbed on silver particles (Figure 2(b)), a band corresponding to ν_s(CO$_2^-$) was observed at 1388 cm^{-1}, instead of a band at 1668 cm^{-1} due to carbonyl ketone (C=O) stretching. Two stretching bands due to (ν_s(NC$_2$)) and (ν_{as}(NC$_2$)) were also measured at 950 cm^{-1} and 1203 cm^{-1}, respectively. The peak shift of an amine group observed at a

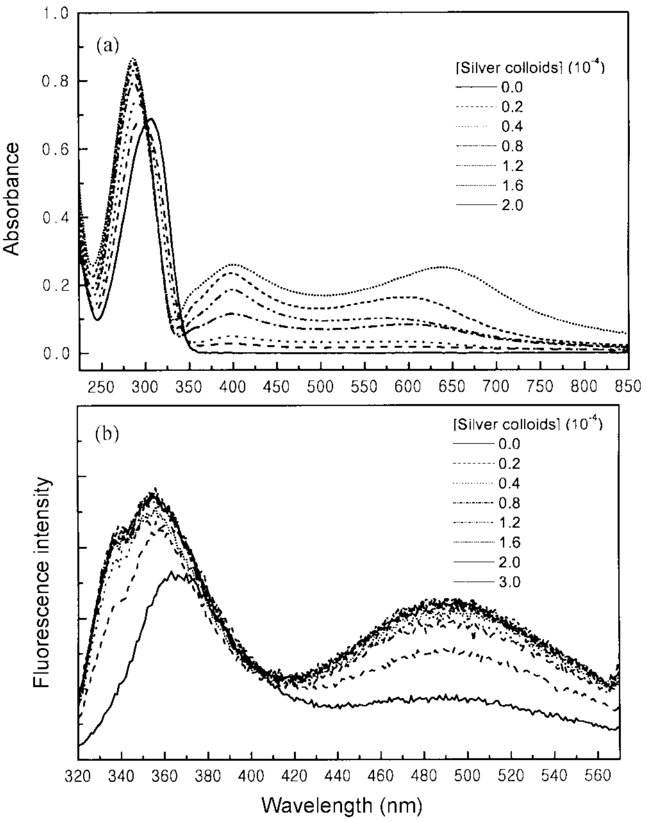

Figure 1. Absorption (a) and emission spectral changes (λ_{ex} = 300 nm) (b) of DMABA with different concentrations of silver colloids.

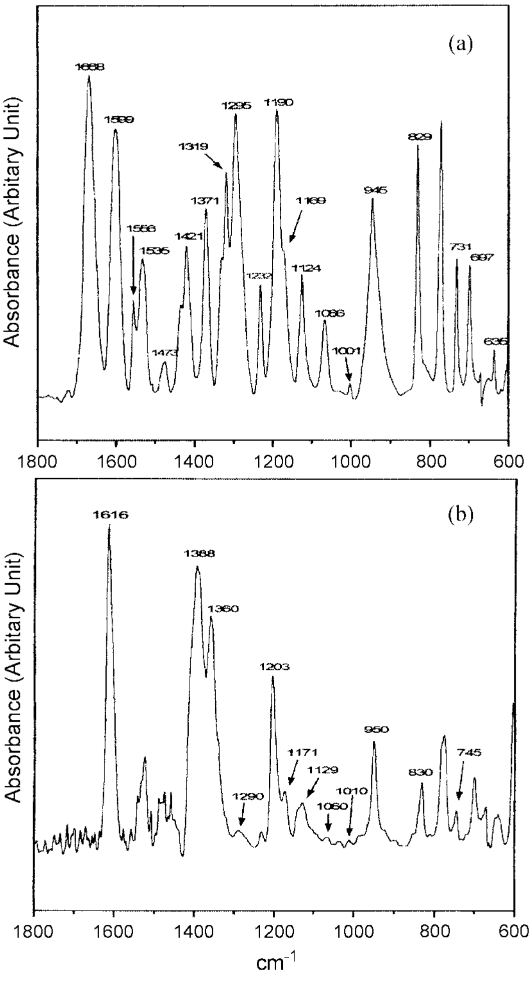

Figure 2. DRIFT spectra of neat DMABA (a) and DMABA adsorbed on Silver colloids (b).

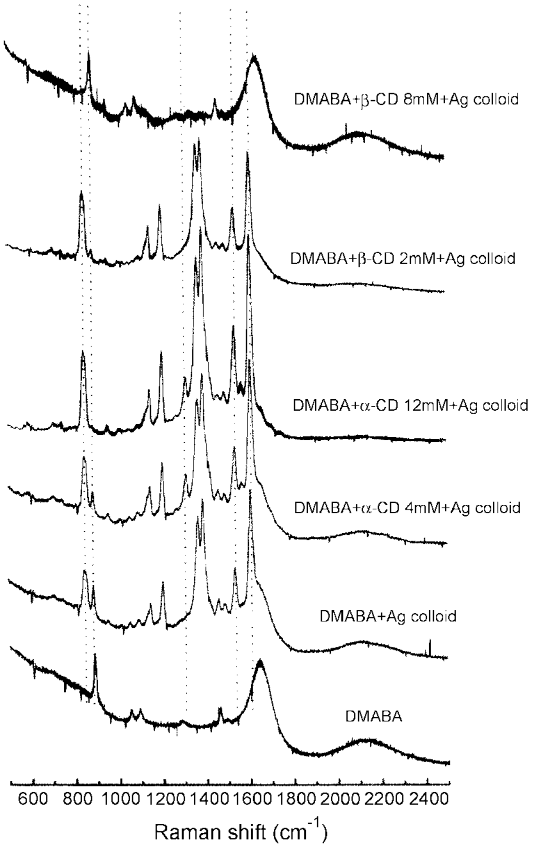

Figure 3. Surface enhanced Raman scattering spectra of DMABA adsorbed on silver colloids in the absence and presence of α-CD or β-CD.

slightly higher wavenumber than that observed in neat DMABA is probably due to the indirect interaction of amino group through the conjugation of DMABA. This indicates that DMABA is adsorbed on silver colloids as a carboxylate form. These characteristic bands of anion form of DMABA are also observed at 1650 nm from the SERS spectrum of DMABA adsorbed on silver colloids in the absence of α-CD or β-CD as shown in Figure 3, supporting again that DMABA is adsorbed on silver colloids as a carboxylate form. Especially, the observation of two bands at 1384 cm^{-1} and 845 cm^{-1} corresponding to $\nu_s(CO_2^-)$ and $\delta(CO_2^-)$, respectively, indicates that the CO_2^- group of DMABA in the ground state is adsorbed through both of its oxygen atoms and π-bonding as a tilted conformation on silver colloids. However, the π-bonding interaction with silver colloidal surfaces is inhibited by the introduction of CD because DMABA molecule is entrapped into the nonpolar cavity of α-CD or β-CD. Especially, in case of β-CD the interaction of DMABA with silver colloids becomes more weak. This is probably because most part of DMABA molecule is deeply entrapped into the β-CD cavity. This is supported by the fact that the SERS of DMABA in the higher concentration of β-CD is the same as that observed in molecules alone (See Figure 3).

In order to further understand the structure of DMABA in the excited-state, we have measured the transient resonance Raman spectra of DMABA adsorbed on silver particles in aqueous α-CD and β-CD solutions. The transient resonance Raman spectra of DMABA adsorbed on silver colloids show similar results regardless of the presence of α-CD or β-CD. Figure 4 shows the transient resonance Raman spectra of DMABA adsorbed on silver colloids in the aqueous β-CD solutions measured with 436 nm photoexcitation and 468 nm probe pluses. The bottom spectrum of Figure 4 was obtained by the probe (468 nm) pulse; the ν_{8a} mode at 1600 cm^{-1}, the ν_{19b} mode at 1450 cm^{-1}, and the $\nu_s(CO_2^-)$ mode at 1380 cm^{-1}, respectively. These vibration modes indicate that DMABA is adsorbed on silver colloids as a carboxylate form as already demonstrated by the DRIFT and SERS spectra. A characteristic change was observed from the transient resonance Raman spectrum of the excited-state DMABA in silver colloidal solutions measured with 436 nm photoexcitation and 468 nm probe pluses (Figure 4(b)). The significant changes for the excited-state DMABA are the disappearance of 1380 cm^{-1} band with appearance of 1280 cm^{-1} band corresponding to $\nu_s(CO_2^-)$ and ν(C-OH) band, respectively. These results imply that the carboxylate group of DMABA adsorbed on silver colloid in the ground-state is recovered to the carboxylic acid group in the excited-state. That is, the carboxylate group of DMABA molecules adsorbed on silver colloids in the excited-state is desorbed from silver colloidal surface in the excited-state. These trends were also observed by Suh *et al.*,[18] demonstrating that 4-vinylbenzoic acid adsorbed on silver colloid surface was desorbed by the laser irradiation and the photodesorption

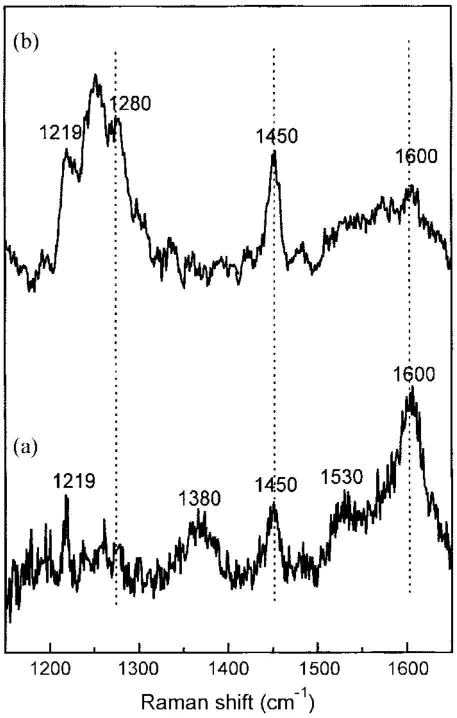

Figure 4. Transient resonance Raman spectra of DMABA adsorbed on silver colloids in the aqueous β-CD solutions measured with 435 nm photoexcitation and 468 nm probe. (a) probe only and (b) pump and probe.

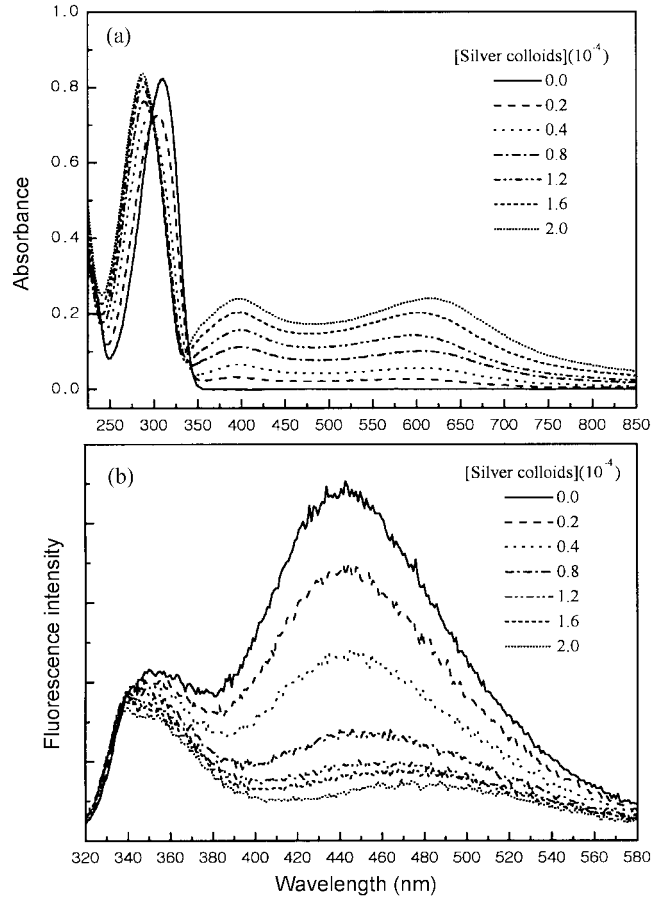

Figure 5. Absorption (a) and emission spectral changes (λ_{ex} = 300 nm) (b) of DMABA/α-CD with different concentrations of silver colloids.

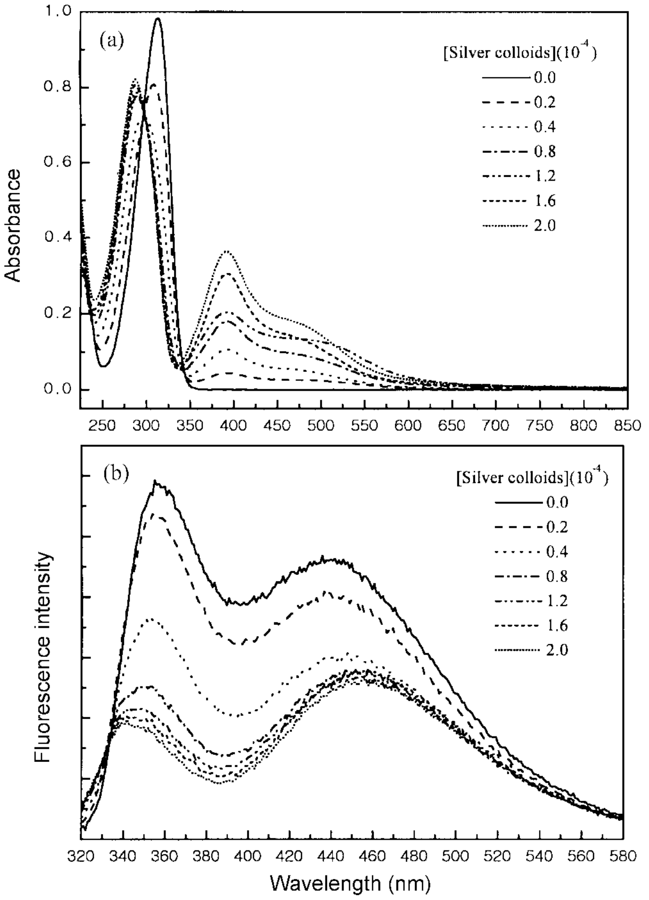

Figure 6. Absorption (a) and emission spectral changes (λ_{ex} = 300 nm) (b) of DMABA/β-CD with different concentrations of silver colloids.

rate constant determined from the changes of the intensity of ν_{8a} vibration mode was proportional to the laser power. They also reported that the photodesorption process was initiated by a metal to adsorbate charge transfer absorption. Especially, in aqueous α-CD and β-CD solutions, the decrease of the intensity of 1600 cm^{-1} corresponding to ν_{8a} mode as well as the disappearance of $\nu_s(CO_2^-)$ band and appearance of ν(C-OH) band was clearly observed as shown in Figure 4, indicating that the photodesorption of DMABA from silver colloid surface takes favorably place in aqueous α-CD and β-CD solutions. Thus, the photorecovered carboxylic acid group of DMABA would be able to lead the hydrogen-bonding interaction with water molecule or the secondary hydroxyl group of α-CD or β-CD.

In order to observe the silver colloid effects on the excited-state intramolecular charge transfer of DMABA, we have also measured the absorption and fluorescence spectra of DMABA in aqueous α-CD and β-CD solutions as increasing the concentration of silver colloids. The absorption and fluorescence spectra of DMABA in aqueous α-CD and β-CD solutions are greatly affected by the presence of silver colloids as shown in Figures 5 and 6. Upon increasing the concentration of silver colloids, the absorption spectra of DMABA entrapped in α-CD cavity are very similar to the absorption spectra of DMABA in aqueous solutions. In contrast to the absorption spectra of DMABA, there are a dramatic changes in the fluorescence behavior of DMABA adsorbed on silver colloids in aqueous α-CD solutions. Upon addition of silver colloids, the emission intensity of DMABA entrapped in α-CD cavity was largely decreased. Especially, the ICT emission (λ_{max} = 440 nm) was greatly rather quenched with little decrease of the normal emission (λ_{max} = 350 nm). In other words, as the concentration of silver colloids increases, the ratio of the ICT emission to the normal emission (I_a/I_b) of DMABA in aqueous α-CD solutions are greatly decreased as shown in Figure 7. It is also noteworthy that the ICT emission maxima are red-shifted by 40 nm upon addition of silver colloids, demonstrating that the most part of DMABA encapsulated in α-CD cavity is exposed to the bulk aqueous solutions by the presence of silver colloids. Thus, in aqueous α-CD solutions, the carboxylic acid group of DMABA in the excited-state can be readily hydrogen-bonded with water molecules, leading to decrease the energy gap between the ICT state and the triplet state. According to energy gap law of nonradiative transitions, the rate of intersystem crossing from the ICT singlet state increases as the singlet-triplet energy gap decreases. That is, the hydrogen-bonding interaction of the carboxylic acid

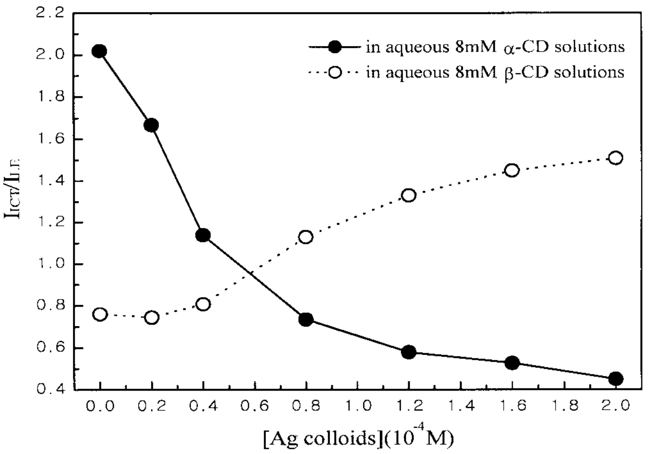

Figure 7. The ratio of the ICT emission to the normal emission (I_a/I_b) of DMABA entrapped in α-CD and β-CD cavity with different concentrations of silver colloids.

group of DMABA with water induces the stabilization of the highly polar ICT state through strong dipole-dipole interaction with water. Consequently, the nonradiative decay from the stabilized ICT state to the ground and/or low-lying triplet state rapidly takes place. Thus, we suggest that the decrease of the I_a/I_b value of DMABA entrapped in α-CD cavity in presence of silver colloids is due to the increase of polarity.

On the other hand, in aqueous 8 mM β-CD solutions, the absorption band arising from DMABA adsorbed on silver colloids is observed at shorter wavelength than that observed in aqueous solutions or in aqueous 8 mM α-CD solutions. This is probably due to the weak interaction of DMABA with silver colloids. Like the absorption spectra of DMABA, the fluorescence behavior of DMABA entrapped in β-CD cavity is greatly affected by the presence of silver colloids. Upon increasing the concentration of silver colloids, the intensity of the normal emission of DMABA entrapped in β-CD cavity was significantly quenched as compared with that of the ICT emission. That is the I_a/I_b values of DMABA in aqueous β-CD solutions are largely increased and the ICT emission maxima are red-shifted by 15 nm upon addition of silver colloids (See Figures 6 & 7). These results suggest that the interaction between DMABA entrapped in β-CD and silver colloids is clearly different from that between DMABA entrapped in α-CD and silver colloids. Especially, the red-shift of ICT emission maxima in aqueous β-CD solutions is smaller than that in aqueous α-CD solutions, indicating that DMABA is still entrapped in the hydrophobic cavity of β-CD. This is probably due to the larger internal diameter of the β-CD cavity than that of the α-CD cavity, leading the guest molecule to be located more deeply into the nonpolar cavity. Thus, DMABA entrapped deeply into the nonpolar β-CD cavity is exposed to the rim of the CD cavity by silver colloids as demonstrated by the small red-shift of the ICT emission. Therefore, in the aqueous β-CD solutions, the carboxylic acid group of DMABA in the excited-state can be readily hydrogen-bonded with the secondary hydroxyl group of β-CD rather than water molecules as shown in Figure 8.

(a) In the ground-state

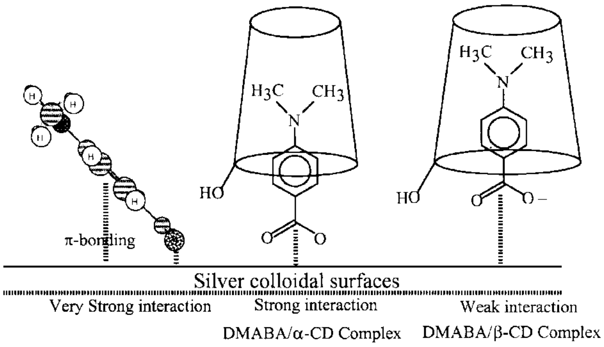

(b) In the excited-state

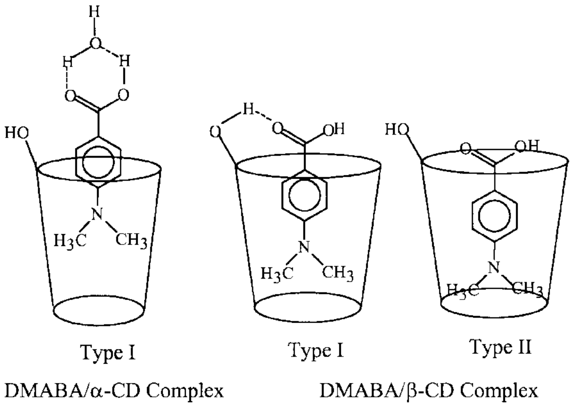

Figure 8. The proposed structures of the DMABA/CD complexes in the ground-state (a) and excited-state (b).

This hydrogen-bonding interaction of the guest molecule with the secondary hydroxyl group of β-CD has been reported by Warner *et al.*[19-21] Thus, this hydrogen-bonding interaction of DMABA with β-CD results in the stabilization of DMABA/β-CD complex. In order to further characterize the interaction between the carboxylate group of DMABA with the secondary hydroxyl group of β-CD, we determined the association constants for DMABA/α-CD or DMABA/β-CD complex from the emission spectra of DMABA in silver colloidal solutions with increasing concentration of α-CD or β-CD. The association constants are determined from the Benesi-Hilderbrand plot by using the following equation;

$$\frac{1}{(I_a/I_b)_0-(I_a/I_b)} = \frac{1}{(I_a/I_b)_0-(I_a/I_b)'} + \frac{1}{K(I_a/I_b)_0-(I_a/I_b)'[CD]}$$

where K is the association constant, $(I_a/I_b)_0$ is the initial ratio of free DMABA, and (I_a/I_b) and $(I_a/I_b)'$ are the observed and intrinsic ratios of the inclusion complex, respectively. Figure 9 shows a straight line from the plot of the reciprocal of $(I_a/I_b)_0-(I_a/I_b)$ *vs* the reciprocal of α-CD or β-CD concentration for the present system, demonstrating 1 : 1 stochiometry in the DMABA/α-CD and DMABA/β-CD complex. From the slope and intercept, the association constants for DMABA/α-CD complex in the absence and presence of silver colloids

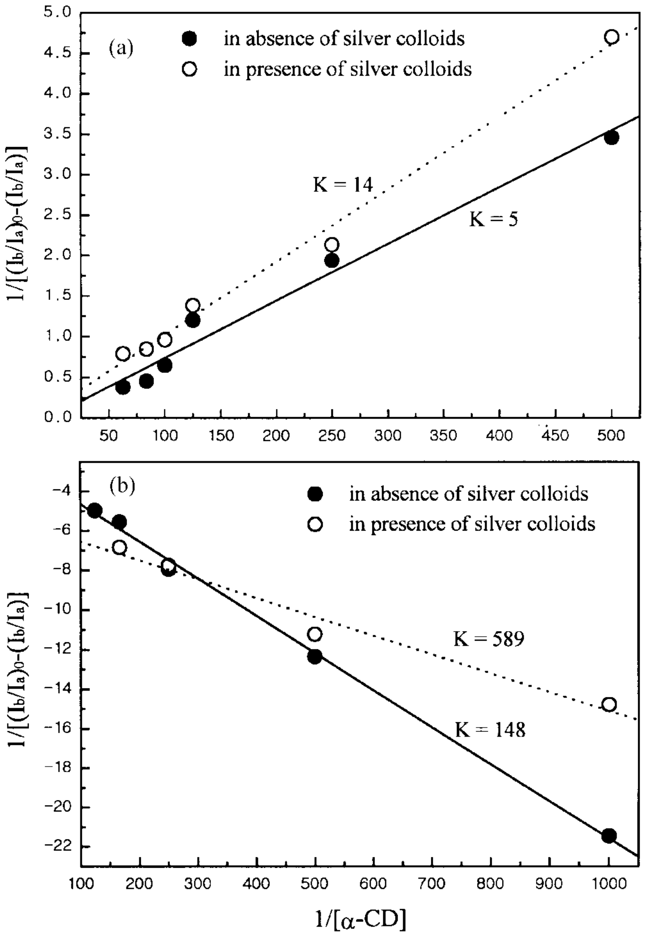

Figure 9. The plot of the reciprocal of $(I_a/I_b)_0-(I_a/I_b)$ *vs* the reciprocal of α-CD (a) and β-CD (b) concentration for the DMABA/CD complex system.

were determined to be 5 and 14 M^{-1}, respectively, indicating that the DMABA/α-CD complex is little affected by the presence of silver colloids. However, the association constant for DMABA/β-CD complex is largely enhanced from 148 to 580 M^{-1} by the presence of silver colloids, indicating that the DMABA/β-CD complex is more stabilized. It is also noteworthy that though DMABA is exposed to the aqueous solutions by silver colloids, the value of the association constant for DMABA/β-CD complex is greatly increased. That is, under the presence of silver colloids, the increase of the association constant for DMABA/β-CD complex arises from the hydrogen-bonding of the carboxylic acid group of DMABA with the secondary hydroxyl group of β-CD. Consequently, in the aqueous β-CD solutions the enhancement of the I_a/I_b value arises from the intermolecular hydrogen-bonding interaction between DMABA with the secondary hydroxyl group of β-CD as well as the lower polarity of the rim of the β-CD cavity compared to bulk water. These results are also consistent with the result reported by Nag *et al.*,[6,22,23] illustrating that the enhancement of the ICT emission obviously originates from DMABN molecules which are in a more polar environment *i.e.* at the rim of β-CD.

In order to further understand the difference in the CD-dependent changes of I_a/I_b value, we measured the fluorescence decay times of the normal (350 nm) and the ICT emission (460 nm) of DMABA in silver colloid solutions containing different concentration of α-CD and β-CD. The analyzed decays of the normal and ICT emission are summarized in Tables 1, 2 and 3. The normal emission decay in the absence of silver colloids exhibits a very fast decay (32 ps) as a major decay component with a small contribution from a slow decay component (0.84 ns). The fast decay component is attributed to the emission from the locally excited (LE) state while the 0.84 ns component corresponds to the delayed emission generated through the equilibration achieved between the LE state and the ICT state. The decay times and their relative amplitudes of the normal emission stay the same within experimental uncertainty even upon addition of silver colloids. Furthermore, two decay components of the normal emission of DMABA adsorbed on silver colloidal surfaces have fairly constant in terms of the decay times and relative amplitudes regardless of the presence of α-CD or β-CD. It is interesting to note that the decays and relative amplitudes of the longer component (0.7 ns) in presence of silver colloids are little affected by the presence of β-CD while those in absence of silver colloids are increased upto 1.6 ns by the presence of β-CD. This decay behavior of the normal emission is consistent with the fluorescence spectroscopic results, demonstrating that as increasing the β-CD concentration, the enhancement of the normal emission in the presence of silver colloids is smaller than that in the absence of silver colloids.

On the other hand, the ICT emission decay of DMABA is also biexponential, exhibiting a fast decay component (230

Table 1. The fluorescence decay times (τ_i) and relative amplitudes (a_i) for the ICT (460 nm) and normal (350 nm) emission of DMABA in the absence and presence of silver colloids

Compounds	Monitoring wavelength	τ_1 (ps)	a_1	τ_2 (ns)	a_2	τ_3 (ns)	a_3	Rise (ps)
Ag coloid-free DMABA	350 nm	32	0.997	0.84	0.003			
DMABA + Ag colloid 10%		35	0.987	0.75	0.013			
Ag coloid-free DMABA	460 nm	235	0.993	1.5	0.007			14
DMABA + Ag colloid 5%		230	0.958			0.47	0.027	20
DMABA + Ag colloid 10%		230	0.969			0.46	0.031	24
DMABA + Ag colloid 15%		233	0.871			0.51	0.129	25

Table 2. The fluorescence decay times (τ_i) and relative amplitudes (a_i) for the ICT (460 nm) and normal (350 nm) fluorescence bands of DMABA adsorbed on silver colloidal surface in aqueous α-CD solutions

Compounds	Monitoring wavelength	τ_1 (ps)	a_1	τ_2 (ns)	a_2	τ_3 (ns)	a_3	Rise (ps)
α-CD-free DMABA	350 nm	35	0.987	0.75	0.013			
DMABA + α-CD 8 mM		32	0.982	0.59	0.014	2.4	0.004	
α-CD-free DMABA	460 nm	230	0.969	0.46	0.031			14
DMABA + α-CD 2 mM		242	0.910			2.3	0.010	31
DMABA + α-CD 4 mM		244	0.972			3.0	0.028	31
DMABA + α-CD 8 mM		247	0.912			3.3	0.088	19
DMABA + α-CD 12 mM		250	0.822			3.4	0.178	20

Table 3. The fluorescence decay times (τ_i) and relative amplitudes (a_i) for the ICT (460 nm) and normal (350 nm) fluorescence bands of DMABA adsorbed on silver colloidal surface in aqueous β-CD solutions

Compounds	Monitoring wavelength	τ_1 (ps)	a_1	τ_2 (ns)	a_2	τ_3 (ns)	a_3	τ_4 (ns)	a_4	Rise (ps)
β-CD-free DMABA	350 nm	35	0.987	0.75	0.013					
DMABA + β-CD 8 mM		32	0.942	0.70	0.028			1.9	0.030	
β-CD-free DMABA	460 nm	230	0.969	0.46	0.031					14
DMABA + β-CD 2 mM		215	0.295			0.89	0.285	1.9	0.420	31
DMABA + β-CD 4 mM		270	0.083			0.81	0.306	1.8	0.611	31
DMABA + β-CD 8 mM		200	0.041			1.0	0.433	1.9	0.526	19

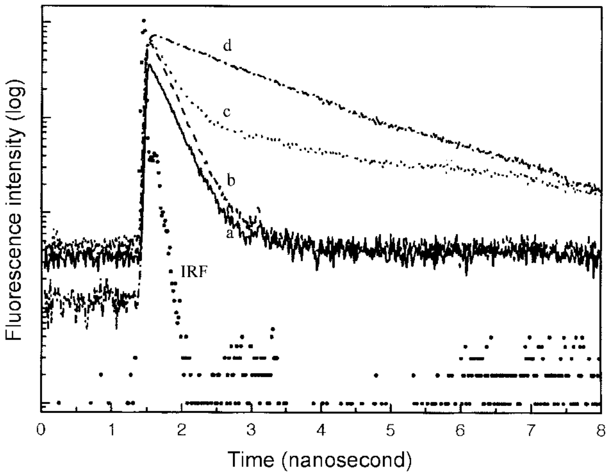

Figure 10. Fluorescence decay profiles for DMABA in aqueous solutions (a), and DMABA adsorbed on silver colloids in the absence (b) and presence of α-CD (c) and β-CD (d).

ps) as a major along with a slow decay component (1.5 ns). Figure 10 shows the typical fluorescence decays for DMABA in aqueous solutions, and DMABA adsorbed on silver colloids in the absence and presence of α-CD and β-CD. The shorter component is attributed to the emission from the stabilized ICT state while the longer component is due to the hydrogen-bonding interaction of DMABA with water. However, upon addition of silver colloids, new decay component (0.47 ns) instead of the longer component is observed while the relative amplitude of the fast component greatly decreases. New decay component is attributed to the emission from DMABA adsorbed on silver colloidal surfaces. Upon addition of α-CD or β-CD, the decay component originating from DMABA adsorbed on silver colloidal surfaces disappear and consequently new decay components become dominant (see Tables 2 and 3), exhibiting much longer decay times (*ca.* 0.9-3.2 ns). Under the presence of silver colloids, the ICT emission for the DMABA/α-CD complex has one decay component (*ca.* 3.4 ns) while that for the DMABA/β-CD complex has two decay components (*ca.* 1.0 and 1.9 ns). This indicates that there are two different species of DMABA/β-CD complex in contrast to a single species of DMABA/α-CD complex as reported by Yoon *et al.* It is noteworthy that the decay times for DMABA/α-CD and DMABA/β-CD complex in the presence of silver colloids are shorter than the those in absence of silver colloids, illustrating that the intensity of the ICT emission is decreased by the presence of silver colloids. As previously mentioned, two different species of DMABA/β-CD complex correspond to the hydrogen-bonding species of DMABA with β-CD (type I) and the type II complex, in which the carboxylic acid group is entirely entrapped in the nonpolar cavity of β-CD. Considering the fluorescence spectroscopic results, demonstrating that with an increase of the β-CD concentration, the I_a/I_b value of DMABA adsorbed on silver colloids initially increases and after reaching a maxima exhibits a constant value(data not shown), 1.0 ns component and 1.9 ns component are attributable to the type I and type II, respectively. These results are consistent with the result reported by Yoon *et al.*, illustrating that at higher concentration of β-CD, the I_a/I_b value of DMABA decreases and the only longer component (*ca.* 3.0 ns) is detected because all the part of

DMABA molecule face nonpolar environment. This is also supported by the fact that only normal emission of DMABA is observed without the ICT emission in the aqueous γ-CD solutions.[2]

From above results, we suggest that the specific hydrogen-bonding interaction of the carboxylic acid group of DMABA with the secondary hydroxyl group of β-CD as well as the hydrogen-bonding between DMABA and water plays an important role in the ICT process.

Conclusions

As the concentration of silver colloids increases, the ratio of the ICT emission to the normal emission (I_a/I_b) of DMABA in aqueous α-CD solutions are greatly decreased while the I_a/I_b values in aqueous β-CD solutions are significantly enhanced and the ICT emission maxima are red-shifted by 15-40 nm. The transient Raman spectra of DMABA in silver colloidal solutions demonstrate that DMABA in the excited-state is desorbed from silver colloidal surface as demonstrated by the disappearance and appearance of 1380 cm^{-1} and 1280 cm^{-1} corresponding to $\nu_s(CO_2^-)$ and ν(C-OH) band, respectively. Thus, in the aqueous β-CD solutions the carboxylic acid group of DMABA in the excited-state can be readily hydrogen-bonded with the secondary hydroxyl group of β-CD because DMABA is entrapped deeply into the β-CD cavity while in aqueous and α-CD solutions the carboxylic acid group of DMABA has the hydrogen-bonding interaction with water. Consequently, in the aqueous β-CD solutions the enhancement of the I_a/I_b value arises from the intermolecular hydrogen-bonding interaction between DMABA and the secondary hydroxyl group of β-CD as well as the lower polarity of the rim of the β-CD cavity compared to bulk water while the decrease of the I_a/I_b value of DMABA entrapped in α-CD cavity in presence of silver colloids is due to the increase of polarity. These results illustrate that the specific hydrogen-bonding interaction of the carboxylic acid group of DMABA with the secondary hydroxyl group of β-CD as well as the hydrogen-bonding between DMABA and water plays an important role in the ICT process.

Acknowledgment. This work has been financially supported by KOSEF through the Center for Molecular Catalysis at Seoul National University.

References

1. Jiang, Y. B. *Appl. Spectrsc.* **1993**, *48*, 1169.
2. Kim, Y. H.; Cho, D. W.; Yoon, M.; Kim, D. *J. Photoscience* **1996**, *3*, 153.
3. Jiang, Y. B. *J. Photochem. Photobiol., A: Chem.* **1995**, *88*, 109.
4. Kim, Y. H.; Cho, D. W.; Yoon, M.; Kim, D. *J. Phys. Chem*. **1996**, *100*, 15670.
5. Cox, G. S.; Hauptman, P.; Turroo, N. *J. Photochem. Photobiol.* **1984**, *39*, 597.
6. Nag, A.; Dutta, R.; Chattopadhyay, N.; Bhattacharyya, K. *Chem. Phys. Letters* **1989**, *157*, 83.
7. Al-Hassan, K. A.; Klein, U. K. A.; Suwaiyan, A. *Chem. Phys. Letters* **1993**, *212*, 581.
8. Kim, Y.; Cheon, H. W.; Song, N. W.; Kim, D.; Yoon, M. *Chem. Phys. Letters* **1997**, *264*, 673.
9. Hashimoto, M.; Hamaguchi, H. *J. Phys. Chem.* **1995**, *99*, 7875.
10. *Surface Enhanced Raman Scattering*; Chang, R. K., Furtak, T. E., Eds.; Plenum: New York, 1982.
11. Suh, J. S.; DiLella, D. P.; Moskovits, M. *J. Phys. Chem.* **1983**, *87*, 1540.
12. Suh, J. S.; Kim, J. *J. Raman Spectrosc.* **1998**, *29*, 143.
13. Jeoung, S. C.; Kim, D.; Cho, D. W.; Yoon, M. *J. Phys. Chem.* **1996**, *100*, 3075.
14. Jeoung, S. C.; Kim, D.; Cho, D. W.; Yoon, M.; Ahn, K. H. *J. Phys. Chem.* **1996**, *100*, 8867.
15. Jeoung, S. C.; Eom, H. S.; Kim, D.; Cho, D. W.; Yoon, M. *J. Phys. Chem.* **1997**, *101*, 5412.
16. Kim, Y. H.; Yoon, M.; Cho, D. W.; Kim, D. *Bull. Korean Chem. Soc.* **1997**, *18*, 803.
17. Creighton, J. A. p314 in Ref 10.
18. Jang, N. H.; Suh, J. S. *J. Phys. Chem. B* **1997**, *101*, 1649.
19. Roberts, E. L.; Dey, J.; Warner, I. M. *J. Phys. Chem.* **1996**, *100*, 19681
20. Dey, J.; Roberts, E. L.; Warner, I. M. *J. Phys. Chem. A* **1997**, *101*, 5296.
21. Dey, J.; Roberts, E. L.; Warner, I. M. *J. Phys. Chem. A* **1998**, *102*, 301.
22. Nag, A.; Dutta, R.; Bhattacharyya, K. *Chem. Phys. Letters* **1988**, *151*, 474.
23. Nag, A.; Dutta, R.; Bhattacharyya, K. *J. Chem. Soc. Faraday Trans.* **1990**, *86*, 53.